REPORT DOCUMENTATION PAGE

Form Approved
OMB No. 0704-0188

1. REPORT DATE *(DD-MM-YYYY)*	2. REPORT DATE	3. DATES COVERED *(From - To)*
27-07-2012	Final Report	Jan 2010 - Jul 2012

4. TITLE AND SUBTITLE
ANALYSIS OF DATA ACQUIRED DURING SHALLOW WATER EXPERIMENTS CONDUCTED IN 2006 AND 2011 (FINAL REPORT)

5a. CONTRACT NUMBER
N00014-10-M-0072

5b. GRANT NUMBER

5c. PROGRAM ELEMENT NUMBER

6. AUTHOR(S)

RAJAN, Dr. Subramaniam D. - Scientific Solutions, Inc.

5d. PROJECT NUMBER

5e. TASK NUMBER
CLIN 0001AB

5f. WORK UNIT NUMBER

7. PERFORMING ORGANIZATION NAME(S) AND ADDRESS(ES)

Scientific Solutions Inc. - 99 Perimeter Rd., Nashua, NH 03063

8. PERFORMING ORGANIZATION REPORT NUMBER
F068-12-0727

9. SPONSORING/MONITORING AGENCY NAME(S) AND ADDRESS(ES)
Office of Naval Research, Code 321 OA
875 North Randolph Street, Suite 1425
Arlington, VA 22203-1995

10. SPONSOR/MONITOR'S ACRONYM(S)
ONR

11. SPONSORING/MONITORING AGENCY REPORT NUMBER

12. DISTRIBUTION AVAILABILITY STATEMENT
Approved for public release. Distribution is unlimited.

13. SUPPLEMENTARY NOTES

14. ABSTRACT

Shallow Water 2006 experiment was conducted in a region off the New Jersey coast where non-linear internal wave activity is known to occur and this resulting in range-dependent sound speed profiles in the water column. In continuation of the work on estimation of range-dependent sediment compressional wave speed profiles, the ability to use data similar to that collected during the shallow water experiment to determine the range-dependent sound speed profiles in the water column due to the presence of internal waves is explored. It is shown that range-dependent sound speed profiles in the water column can be obtained assuming that the sediment characteristics are known. During 2011 a series of experiments were conducted off the coast of New Jersey. The primary objective of this experiment was to evaluate the possibility of determining the sediment acoustic properties by the use of air launched sonobuoys such as those used ASW operations. It is shown that such a system can be used to extract the sediment acoustic properties.

15. SUBJECT TERMS

Characterization of internal waves, Inverse problem, Modal inverse

16. SECURITY CLASSIFICATION OF:			17. LIMITATION OF ABSTRACT	18. NUMBER OF PAGES	19a. NAME OF RESPONSIBLE PERSON
a. REPORT	b. ABSTRACT	c. THIS PAGE			Dr. Subramaniam D. Rajan
U	U	U	SAR	31	19b. TELEPONE NUMBER (*Include area code)* (603) 880-3784

SCIENTIFIC SOLUTIONS, INC.
INNOVATIVE RESEARCH AND ENGINEERING

UNCLASSIFIED

(Approved for public release. Distribution is unlimited.)

SSI Contractor Report: F068-12-0727

ANALYSIS OF DATA ACQUIRED DURING SHALLOW WATER EXPERIMENTS CONDUCTED IN 2006 AND 2011 (FINAL REPORT)

Principle Investigator:
Dr. Subramaniam D. Rajan, SSI

Scientific Solutions, Inc.
99 Perimeter Road
Nashua, NH 03063-1325

Prepared for

Office of Naval Research
Kyle Becker, PhD Code: 321OA
Office of Naval Research (ONR)
875 North Randolph Street, Suite 1425
Arlington, VA 22203-1995
under Contract No: N00014-10-M-0072 – CLIN 0001AB
POP: January 2010 – July 2012

July 2012

UNCLASSIFIED

ANALYSIS OF DATA ACQUIRED DURING SHALLOW WATER EXPERIMENTS CONDUCTED IN 2006 AND 2011

Office of Naval Research
Contract No: N00014-10-C-0072 – CLIN 0001AB

ABSTRACT

Shallow Water 2006 experiment was conducted in a region off the New Jersey coast where non-linear internal wave activity is known to occur and this resulting in range-dependent sound speed profiles in the water column. In continuation of the work on estimation of range-dependent sediment compressional wave speed profiles, the ability to use data similar to that collected during the shallow water experiment to determine the range-dependent sound speed profiles in the water column due to the presence of internal waves is explored. It is shown that range-dependent sound speed profiles in the water column can be obtained assuming that the sediment characteristics are known.

During 2011 a series of experiments were conducted off the coast of New Jersey. The primary objective of this experiment was to evaluate the possibility of determining the sediment acoustic properties by the use of air launched sonobuoys such as those used ASW operations. It is shown that such a system can be used to extract the sediment acoustic properties.

ANTICIPATED BENEFITS:

The methods can be adopted to characterize the range dependent environment namely the water column and the sediment.

KEYWORDS:

Characterization of internal waves, Inverse problem, Modal inverse

TABLE OF CONTENTS

LIST OF FIGURES

1.0 BACKGROUND

During the first year of work done under this contract, the main objective was to investigate approaches to estimating the range dependent structure of sound speed profiles in the water column. It is known that the sound speed profiles of the water column vary in space and time. One of the causes for this variation in sound speed profiles is the presence of internal waves. Here we investigate the estimation of the water column sound speed profiles from data collected using a narrow band/broad band source.

We examine two methods for estimating the range dependent water column sound speed profiles from acoustic data collected in the water column. First we adopt extended Kalman filter [1] and estimate the sound speed profiles in the water column in a sequential manner with the arrival of each new acoustic data. In the second method we estimate the variability in the water column sound speed profiles based on the variation in travel time of modes as was done for estimating the range dependence of sediment compressional wave speed profiles [2].

During the second year of the contract, the emphasis shifted to analysis of data collected during an experiment conducted in 2011. The ultimate objective of this experiment is to transfer technology developed for estimating sediment acoustic properties using modal data as a research initiative in to an operational tool where in air launched sonobuoys will used to collect data for further processing and estimation of sediment acoustic properties. Analysis of the data collected during the experiment shows that this is an achievable goal.

2.0 SCIENTIFIC/TECHNICAL OBJECTIVE

For obtaining the range-dependent sound speed profiles of the water column we use two methods one based on extended Kalman filter and the other based on variation in modal travel time. We evaluate both these methods using simulated data. The acoustic source for the experiment will be broad band source with adequate band width. The signal acquired by the receivers on vertical array or at a spatially distributed set of receivers will be used to estimate the range dependent sound speed profiles of the water column. A more detailed description on this work is found in our progress report submitted last year [3]. The salient points of the work are outlined in the next section.

The data collected during the 2011 experiment after processing yielded the pressure field which is a function of range at a set of frequencies. This was transformed to determine the wave number spectrum and from it the eigenvalues of propagating modes. These values are the input to the inversion scheme for extracting the sediment properties. The basic question to be answered in this analysis is whether the commercially developed sonobuoys for use by the Navy have the performance capability (a) for acquiring the pressure field and GPS data and (b) for transmission of the data to the base station. This capability will determine the ability of this operational scheme to estimate the sediment acoustic properties.

3.0 ESTIMATION OF SOUND SPEED PROFILE OF WATER COLUMN IN A RANGE-DEPENDENT ENVIRONMENT

3.1. APPLICATION OF EXTENDED KALMAN FILTER

The model for the water column variability adopted in [4] is chosen to simulate the range dependent nature of the sound speed profiles in the water column. The range dependent sound speed profile is determined as a sum of a background sound speed profile plus a range dependent variation that is the result of internal wave activity. The environment is specified with range-independent fluid sediment properties and a constant water/sediment interface depth of 200 m. The seabed has a compressional wave speed of 1700 m/ s, a density of 1.5 g/cm3, and an attenuation of 0.1 dB/λ. Density in the water column is 1 g/cm3 and no attenuation.

The range dependent nature of the sound speed structure in the water column is shown in Figure 3.1.1.

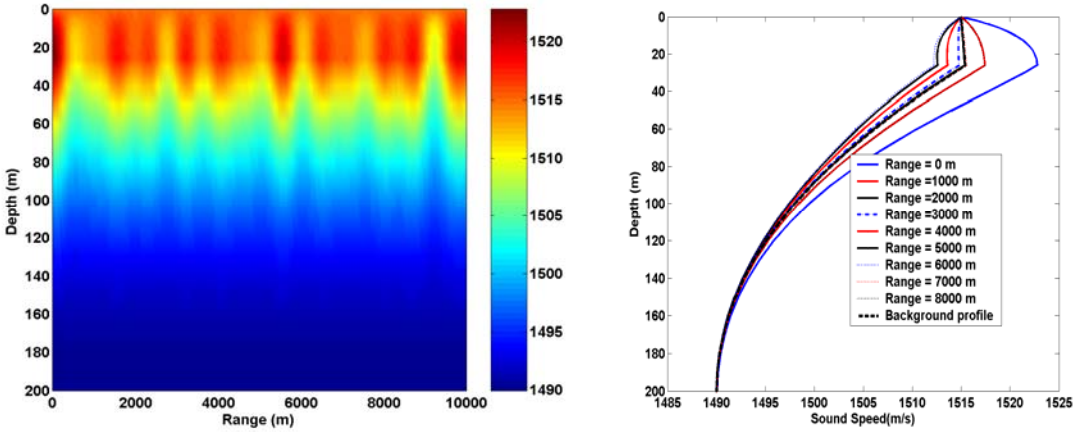

Figure 3.1.1. The left panel shows the variability in the sound speed profiles as a function of range and depth. The right panel shows the sound speed profiles at a discrete set of ranges together with the background profile.

Our basic assumption in applying Kalman tracking approach to the estimation of the sound speed profiles is that the variability in the sound speed profile is due to the propagation of an internal wave field. Therefore the each range location refers to a time in the propagation of the internal wave field. We, therefore, use acoustic data collected on a vertical array as a function of time to estimate the sound speed structure in the water column. Assuming that the internal wave travels at a speed of 1.0 m/s it will travel 1000 m in 1000 seconds or approximately 17 minutes. Therefore by collecting the acoustic data on a vertical array at much smaller time steps say at one minute intervals one can estimate the variability caused to the water column sound speed structure as the internal wave field moves along. In order to estimate the sound speed profile in the water column as a function of time we use the extended Kalman filter as outlined in [1].

3.1.1. Sound Speed Parameterization

The sound speed in the water column is obtained by using empirical orthogonal functions. Then for any sound speed profile its deviation from the mean can then be represented as a linear combination of the EOFs as shown below.

$$\delta C = \boldsymbol{E}\ \alpha \tag{1}$$

where $\boldsymbol{E}$ is a matrix containing the Eigen vectors or the EOFs and α is a vector of EOF coefficients. Using the orthogonal property of the EOFs we can determine the coefficients α. In most cases any realization of the sound speed profile can be obtained by a linear combination of a small number of EOFs. Therefore only a small number of EOF coefficients are required to be determined in order to estimate the speed profile.

In estimating the range-dependent sound speed profiles we divide the region between the source and receiver into J non-overlapping regions. The SSP in each region is given by the following expression.

$$C(r_j, z) = \overline{C}(z) + \sum_{l=1}^{L} \alpha_{jl} E_l \tag{2}$$

where $\overline{C}(z)$ is the mean profile, α_l is the lth EOF coefficient and E_l is the lth EOF.

3.1.2. Formulation Using Extended Kalman Filter

Let us consider an experimental configuration where a receiver array is placed at a range R from a source transmitting a CW signal acquires data. The region between the source and the vertical array is divided in to J regions. The signal is transmitted repeatedly with a delay of T seconds between transmissions. We also assume that prior to the start of the transmission there are no internal wave activity in the ocean. The ocean sound speed at this time is range independent. With the internal wave propagating through the region between the source and receiver, the sound speed structure becomes range-dependent. For simplicity we assume that between the transmission of the first and second signal the sound speed structure in the Region 1 changes with the rest of the space between the source and receiver having a range independent SSP that existed in the area prior to the propagation of the internal wave field. Similarly between the first and the third transmission, the Regions 1 and 2 have different SSP due to the propagation of the internal wave field and the rest of the regions will have SSP that existed before the propagation of the internal wave field. Therefore by analyzing the data acquired at the vertical array we attempt to estimate the SSP in the regions sequentially.

We relate the data to the parameters we estimate through the equation

$$\begin{pmatrix} P(R,z_1) \\ \vdots \\ \mathrm{P(R,z_M)} \end{pmatrix} = \Phi(\alpha) + \nu \tag{3}$$

where $P(R, z_m)$ is the acoustic pressure at the mth element of the vertical array placed at a range R from the source and Φ represents the nonlinear function of the vector α containing the EOF coefficients which predicts the acoustic pressure at the receiver. The EOF coefficients are used to compute the sound speed structure in the water column which is then an input to a propagation algorithm such as RAM [5] that computes the acoustic pressure at the elements of the vertical array. Let $\boldsymbol{R}_{ww}$ and $\boldsymbol{R}_{vv}$ be the error covariance matrix for model parameter vector α and the measured data respectively. The length of the vector α depends on the number of regions for which the EOF coefficients are estimated. If the number of EOFs used to compute the SSP is N for each region and if there are J regions for which we are estimating the EOF coefficients, the length of the vector α is N×J.

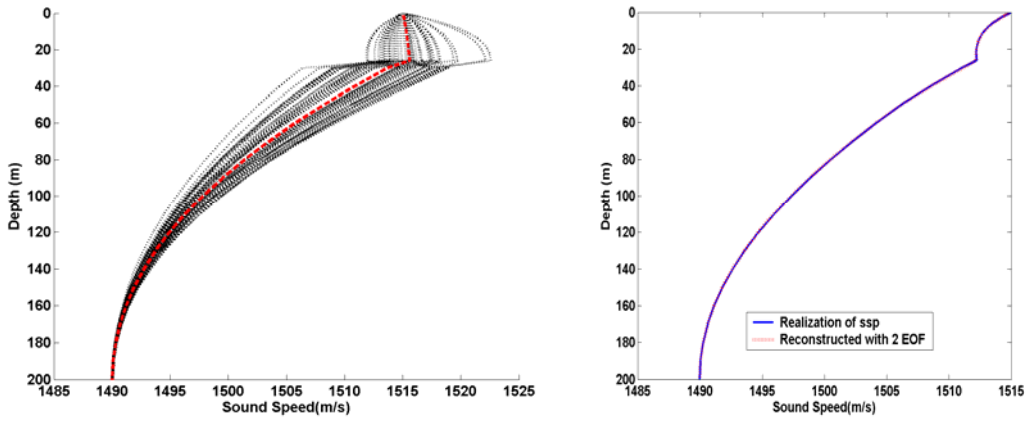

Figure 3.1.2. The realization of the sound speed profiles and the mean profile is shown in the left panel. The true profile and the reconstructed profile using only two EOFs are shown in the right panel.

Using the approach of extended Kalman filter, a new estimate of the EOF coefficient vector is obtained. The new estimate of the EOF coefficients is now used to predict the sound speed profile in the region considered.

3.1.3. Results of Simulation Study

The procedure outlined above is tested using simulated data. For this experiment we assume that the sound speed structure of the water column is range-dependent. At time zero the sound speed

profile in the water column is range independent. At the end of the first time interval the sound speed profile in the first 1000 m from the source changes while the rest of the region remains unchanged. At the end of the second time interval the sound speed structure in the region 1000 m to 2000 m also changes. This proceeds in a similar fashion when finally the entire region between the source and receiver changes from the initial background profile. These changes we attribute to the propagation of an internal wave field from source location towards the receiver position.

The procedure outlined in the previous section was used to estimate the sound speed profiles sequentially for the different regions. In order to perform the estimation as outlined above a set of EOFs were obtained by generating 50 realizations of the sound speed profile Using this set of profiles a mean profile is first obtained. The deviation of each of this realization from the mean profile is used to create the covariance matrix and then by Eigen analysis of the covariance matrix the EOFs are determined. Only three EOFs are required to reconstruct the sound speed profiles without significant error.

The estimation of the sound speed profiles was performed sequentially. First the sound speed profile in Region 1 was determined. To perform this estimation an initial estimate of the EOF coefficients is needed. In order to obtain an initial value of the EOF coefficients we compute the acoustic field at the vertical array with each of the 50 realizations of sound speed as the sound speed in Region 1. The rest of the medium is assumed to have the known ambient sound speed profile. Then the sound speed profile for which the field at the vertical array is close to the value measured in the field experiment is selected and the EOF coefficient corresponding to this sound speed profile is used as the initial estimate of the EOF coefficients. Then corrections to this value of the EOF coefficients were obtained iteratively. Then the value of the sound speed profile for the region was obtained. This procedure is followed for determining the initial value of EOFs and the corresponding sound speed profiles for other sections.

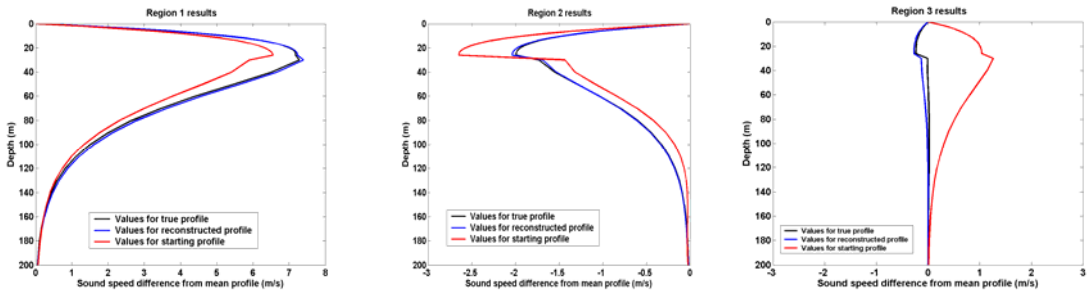

Figure 3.1.3. The three panels show the results of the estimation for the first three regions (Regions 1 to 3). The plot in each panel shows (a) the difference between the true sound speed profile and the mean profile (full line in black), (b) the difference between the true profile and the initial profile (full line in red) and (c) the difference between the true profile and the reconstructed profile (full line in blue). All these are plotted against depth.

3.2. INVERSIONS BASED ON MODE TRAVEL TIME

In [2] we have described an approach for estimating sediment compressional wave speed in the sediment in a range dependent environment. The same approach can be used to determine the range dependent sound speed profiles in the water column. The experimental set up has a broadband source transmitting the signal. A receiver placed at some distance from the source acquires the signal. By using a multiplicity of sources and receivers we obtain a set of signals corresponding to each source/receiver combination. Spectrogram analysis of the received signals gives an estimate of the travel times for each mode at different frequencies along the paths of each source/receiver combination. These data are the input to the inversion algorithm.

3.2.1. Demonstration of the Approach Using Simulated Data

In this demonstration of a method based on mode travel time perturbations we look at the propagation on non-linear internal waves. These types of internal often occur in coastal area. The displacement of a packet of solitons is shown in the left panel of Figure 3.2.1. The sound speed perturbations due to the presence of these solitons are shown in the right panel of Figure 3.2.1. The solitons were simulated based on the procedure in [6].

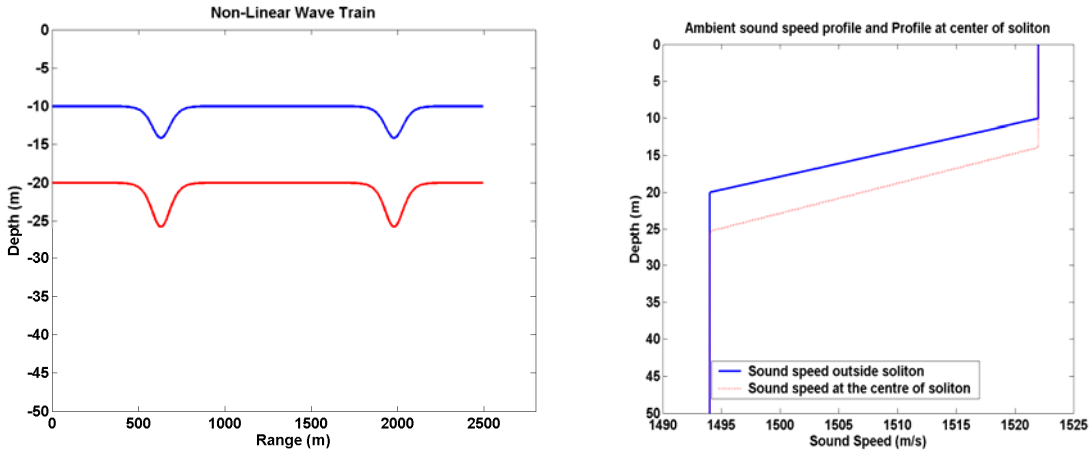

Figure 3.2.1. The left panel shows the propagation of a train of solitons. The right panel shows the sound speed profile outside the soliton and in the center of the solitons.

The experimental geometry consists of one source transmitting a broadband signal. Three receivers are placed at approximately 10,000 meters from the source as shown in the left panel of Fig. 3.2.2. The acoustic path from the source to the receivers goes through the solitons. The mode travel time will be affected by the presence of the solitons. The right panel of Fig. 3.2.2. shows the group velocity of mode one in the region outside the soliton and for an environment defined by the sound speed profile at the center of the soliton.

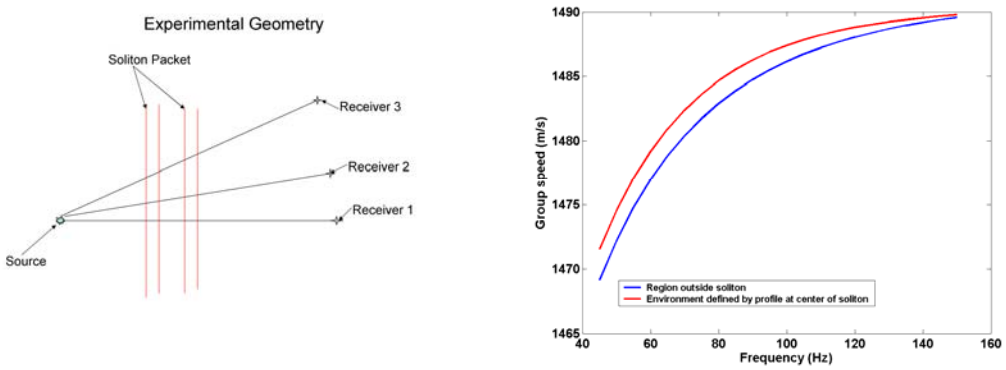

Figure 3.2.2. The left panel shows the experimental configuration used for the simulation study. The right panel shows the group speed as a function of frequency for a region defined by the sound speed profile outside the soliton and an environment defined by the profile at the center of the soliton.

Our aim is to estimate the sound speed structure within the soliton from mode dispersion data. All other parameters (i.e. the sediment acoustic parameters) are assumed known. The sediment layer was 50 m thick with the compressional wave speed of 1700 m/s, density of 1.5 gm/cc and an attenuation of 0.1 dB/λ. This is followed by a infinite half space where the compressional wave speed is 1800 m/s density of 1.5 gm/cc and attenuation of 0.1 dB/λ. Further we treat the sediment as a fluid and ignore any shear effects.

In first set of experiments we assumed that the shape of the soliton as an inverted hat so the sound speed structure within the soliton remained the same. We further assumed that there was no mode coupling due to the range dependence and computed the mode travel time from the group speed for the two environments namely one representing the region outside the soliton and the other one within the soliton. So if υ_{g1} is the group speed in region outside the soliton and υ_{g2} is the group speed within the soliton, then the mode travel time is $\frac{L_1}{\upsilon_{g1}} + \frac{L_2}{\upsilon_{g2}}$ where L_1 and L_2 are the acoustic path lengths outside the soliton and within the soliton respectively. The sound speed structure for the regions outside and inside the soliton are shown in the right panel of Fig. 3.2.1.

3.2.2. Estimation of Sound Speed Profiles

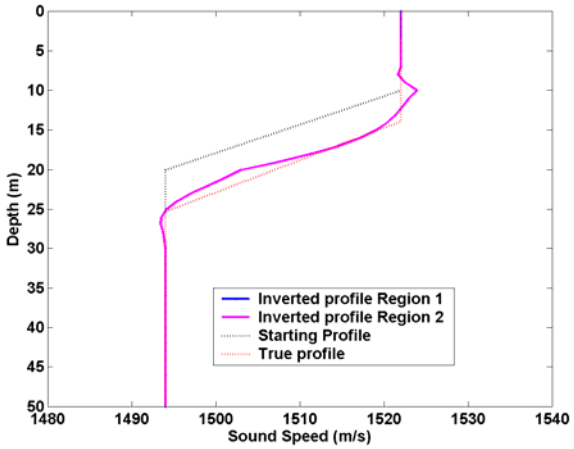

Figure 3.2.3. The reconstructed profile for the sound speed within the soliton for the two locations of the solitons. The staring profile was the sound speed profile outside the soliton region which we considered as known as this can be measured prior to the propagation of the internal waves through the experimental area. The figure shows the inverted profile for both the regions.

We consider the experimental configuration in Fig. 3.2.1. where the range dependence is caused by soliton train with a different compressional wave speed profile. If we know the locations of the ranges at which the soliton occurs then the acoustic path lengths L_{ij}, i=1, 2, 3 and j=1, …., 5 are obtained without error. The mode travel time data and the distances L_{ij} along each source/receiver path are then used to estimate the sound speed profiles within the soliton region.

The inverted profile for the sound speed in the soliton region is shown in Fig. 3.2.3. The result was obtained after imposing constraint on the solution using regularization. The inverted profile is in good agreement with the true profile. Deviations from the true profile are the result of the constraints imposed on the solution.

In a field experiment the travel time of the modes are estimated from the spectrogram analysis of the broad band signals acquired at the receivers. In our simulation of the experiment we used a single source and three receivers as shown in Fig. 3.2.2. The signal used in simulations was a linear frequency modulated signal in the band 40 Hz to180 Hz. The signal duration was 0.2 seconds with a sampling frequency of 5000 Hz. This, therefore, provided adequate resolution in the time domain to be able to determine the perturbations in mode travel times that occur due to the presence of solitons.

The soliton train was modeled as shown in the left panel of Fig. 3.2.1. The sound speed profile at the center of the soliton is shown in the right panel of Fig. 3.2.1. The sound speed profile varied linearly from its value outside the soliton to the value at the center and then back again to the

value outside the soliton region. The mode travel times are obtained from the spectrograms of the signals at the three receivers.

Propagation through a soliton packet has been studied by many investigators and it has been reported that the presence of solitons can cause mode coupling. The possibility of mode coupling in the model of soliton used in the simulation model was investigated and it was noticed that the mode coupling had minimal effect on higher order modes and even in the case of lower order modes its impact on mode ravel times was minimal. In view of these results, the soliton model which uses the sound speed profile in Fig 3.2.4. as occurring in the center of the soliton was used.

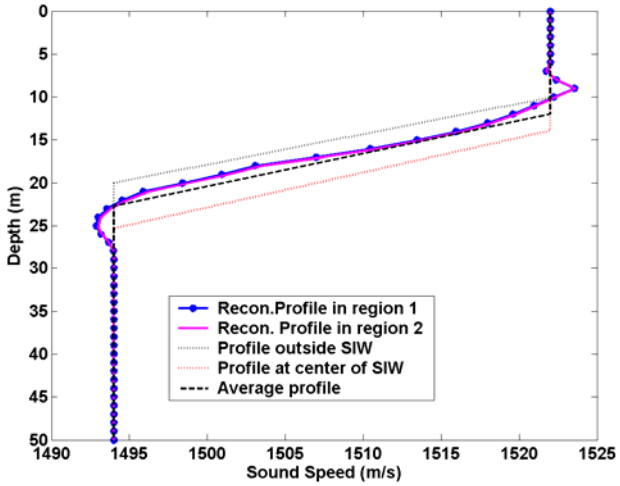

Figure 3.2.4. The sound speed profile with the soliton region as obtained by inversion is compared with the profile at the center of the soliton and an average profile which is the average profile over the entire soliton region.

The mode arrival time as a function of frequency was extracted from the spectrogram analysis of the signals from the three source-receiver paths. This was then used in the inversion algorithm to determine the sound speed profile within the soliton. The reconstructed profiles for the two soliton regions are shown in Fig. 3.2.4. The figure shows the inverted profile together with the starting profile, the profile at the center of the soliton and an average profile that is the average sound speed profile over the entire soliton width. We notice that the inverted profile which represents the sound speed within the soliton gives an estimate that is close to the average profile and not to the value at the center of the profile. This is because in the inversion algorithm the region within the soliton was modeled as one range independent region and the result of inversion therefore provides a range averaged value of sound speed within the region.

As a further check on the validity of the results the mode travel time used as data are compared with the mode travel time for the inverted profile and it was observed that the mode travel times from the inverted model agrees with the data used in the inversion except for some minor discrepancies.

4.0 ESTIMATION OF SEDIMENT ACOUSTIC PARAMETERS USING AIR LAUNCHED BUOYS

4.1. BACKGROUND

Sonobuoys are deployed from air in support of ASW operations and their primary mission is to be able to locate enemy submarines or other enemy ships. The sonobuoys work in passive/active listening mode. Techniques that were relevant in the past for localizing the sonobuoys once deployed were inaccurate, time consuming and involved air craft maneuvers in the vicinity of the buoys. With the advent of GPS systems the buoys are now being equipped with GPS devices. The sonobuoy can therefore transmit their GPS locations to the aircraft. The operational environment for GPS on the buoys is more arduous. The antenna from the sonobuoy does not project far above the surface of the water and is affected by wave action. Therefore, though the GPS system for other applications has been in use for long, the development of GPS for sonobuoys have been taken up only in recent years.

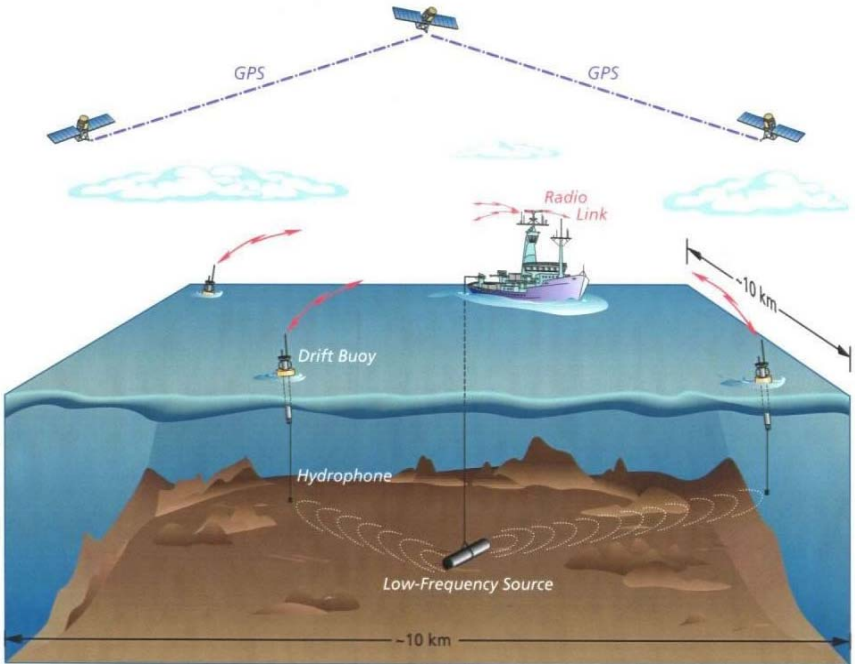

Figure 4.1.1. Schematic of Modal Mapping Experiment illustrating distribution of freely drifting buoys equipped with hydrophones and GPS. The data are transmitted over VHF radio to the ship for storage and analysis. In an operational context, deployment and data processing would take place from an aircraft.

Over the last 20 years a number of experiments (Modal Mapping Experiments (MOMAX)) were conducted. The idea behind these experiments was on the notion that the relative motion between freely drifting buoys making up an active acoustic system of source and receivers will create a synthetic aperture. Figure 4.1.1 shows a schematic of the modal mapping experiment. Applying

appropriate signal processing techniques, the measured data can be transformed into the modal wave number domain (the spatial equivalent of the frequency domain). The modal wave number data then form the basis for an inversion algorithm to estimate compressional wave speed in the underlying sediments. The latest in this series of experiments is MOMAXV which was conducted in March 2011.

During MOMAXV two sets of sonobuoys were deployed namely sonobuoys developed at Woods Hole Oceanographic Institution for the earlier MOMAX experiments and a commercially developed model Ultra Electronics model AN/SSQ53F. During the experiment, both MOMAX and Ultra Electronics model AN/SSQ 53F sonobuoys equipped with GPS were deployed. Similar to the original MOMAX buoys, the commercial SSQ 53F buoys were equipped with an omni-directional hydrophone (in addition to a directional hydrophone pair), GPS navigation, and radio telemetry. Unlike the MOMAX buoys, the SSQ 53F buoys are designed to be launched by aircraft. As configured in the operational role, once the buoy hits the water, a float inflates bringing the buoy back to the surface while the hydrophone pays out to a pre-selected depth. Once at the surface, the buoy sends data back over a VHF radio link. The float itself contains both the VHF and GPS antennae. The objectives for this trial were to compare acoustic data and the transformed wave number estimates, along with inversion results, obtained using the two systems. More generally, an objective was to determine whether inversion methodologies developed in the basic research community could be transitioned and used with operational assets.

4.2. FORMULATION OF INVERSION APPROACH

It can be shown that in a range independent circular symmetric ocean, the wavenumber spectrum $G(k_r,\omega)$ at radian frequency ω and the pressure fields $p(r,\omega)$ at a range r due to a harmonic point source of the same frequency are related by the equation [7]

$$p(r,\omega) = \int_0^\infty G(k_r,\omega) J_0(k_r r) k_r dk_r \tag{4}$$

where k_r is the horizontal wavenumber, and J_0 is the Bessel function of order zero. The inverse of this relation yields the wavenumber spectrum from the pressure field

$$G(k_r,\omega) = \int_0^\infty p(r,\omega) J_o(k_r r) r dr \tag{5}$$

In the far field, the argument $k_r r$ has large values and we can use the asymptotic approximation for the Bessel function.

$$J_0(k_r r) \approx \frac{\exp\left[i\left(k_r r - \pi/4\right)\right]}{\sqrt{2\pi k_r r}}, k_r r >> 1 \tag{6}$$

Insertion of this approximation in (5) yields the following relationship for the wavenumber spectrum.

$$G(k_r,\omega) = \frac{\exp(-i\pi/4)}{\sqrt{2\pi k_r}} \int_0^\infty \sqrt{r}\, p(r,\omega) \exp(-ik_r r) dr \tag{7}$$

For any given ω the wavenumber spectrum $G(k_r,\omega)$ has peaks whose locations on the wavenumber axis are the modal wavenumbers of the propagating modes at that ω. The modal wavenumbers of the propagating modes in a shallow water waveguide are dependent on the acoustic and geometric parameters of the shallow water environment.

Rajan et. al [8] describes a scheme where in modal wavenumbers obtained from a field experiment can be used to estimate the sediment acoustic properties which are briefly described here. The wavenumbers of the propagating modes in the wave guide are obtained from the wavenumber spectrum. Let k_n be the wavenumber of the nth mode as obtained from field measurement of the pressure field. Let us assume that the unknown quantities are the compressional wave speed in the sediment layers. All other parameters of the sediment layers and the water column are assumed known. We now assume that the compressional wave speed profile representing the sediment layers is given by $C_b(z)$. This initial estimate is normally obtained from archival data or other sources of information. Let this initial estimate be related to the true but unknown compressional wave speed profiles by the equation $C(z) = C_b(z) + \Delta c(z)$ where $\Delta C(z)$ is a small quantity which is the difference between the initial estimate of the compressional wave speed profile and the true profile. By solving the forward problem we determine modal wavenumbers for the initial ocean model. Let these be k_{bn}. In a range independent ocean environment, the difference Δk_n between the wavenumbers obtained from the field measurements and the wavenumbers corresponding to the assumed ocean model are related to $\Delta C(z)$ by the integral equation [8]

$$\Delta k_n = \frac{1}{k_{bn}} \int_0^\infty \frac{\omega^2 \Delta C(z)}{C_b^3(z)\rho(z)} \left|U_{bn}(z)\right|^2 dz \tag{8}$$

In the above equation, which is obtained by a linearizing process, $U_{bn}(z)$ is the eigenfunction of the nth mode for the assumed ocean model, and ρ is the known density of the sediment layers. By solving this integral equation we can obtain the quantity $\Delta C(z)$ and hence the true compressional wave speed profile. Since the integral equation is non-linear, the solution is obtained iteratively.

Let us now consider an ocean model in which the medium is represented as comprising homogeneous layers i.e. the compressional wave speed in each layer is a constant. Let there be M sediment layers. We can then write (8) as

$$\Delta k_n = \frac{1}{k_{bn}}\left[\int_0^{z_1} \frac{\omega^2 \Delta C_1}{C_{b1}^3 \rho_1}\left|U_{bn}(z)\right|^2 dz + \cdots + \int_{z_{M-1}}^{z_M} \frac{\omega^2 \Delta C_M}{C_{bM}^3 \rho_M}\left|U_{bn}(z)\right|^2 dz\right] \qquad (9)$$

In the above expression the quantities ρ_m and C_{bm} are the density and the initial estimate of the compressional wave speed in the mth layer, and ΔC_m is the correction to the compressional wave speed in the mth layer that we seek to determine. For a set of N modal wavenumbers, (9) can be represented by the matrix equation

$$\Delta \boldsymbol{k} = \boldsymbol{A}\Delta \boldsymbol{C} \qquad (10)$$

where $\Delta \boldsymbol{k}$ is a vector containing the wavenumber differences for N modes, $\Delta \boldsymbol{C}$ is a vector of length M containing the corrections to the compressional wave speed for the M layers and $\boldsymbol{A}$ is an NxM matrix whose element A_{nm} is given by the expression

$$A_{nm} = \frac{1}{k_{bn}} \int_{z_{m-1}}^{z_m} \frac{\omega^2}{C_{bm}^3 \rho_m}\left|U_{bn}(z)\right|^2 dz \qquad (11)$$

The element A_{nm} represents the change in the modal wavenumber of the nth mode due to unit change in the compressional wave speed in the mth layer. If data from a set of frequencies are used the integral equation (8) is replaced by a set of equations as shown below to incorporate multi-frequency inversion:

$$\Delta k_n(\omega_p) = \frac{1}{k_{bn}(\omega_p)} \int_0^{\infty} \frac{\omega_p^2 \Delta C(z)}{C_b^3(z)\rho(z)}\left|U_{bn}(z)\right|^2 dz, n = 1, \cdots, N, \;\; p = 1, \cdots, P \qquad (12)$$

This set of integral equations is reduced to a matrix equation of the form

$$\begin{bmatrix} \Delta \boldsymbol{k}(\omega_1) \\ \hline \bullet \\ \hline \bullet \\ \hline \bullet \\ \hline \Delta \boldsymbol{k}(\omega_{\boldsymbol{P}}) \end{bmatrix} = \begin{bmatrix} \boldsymbol{A}(\omega_1) \\ \hline \bullet \\ \hline \bullet \\ \hline \bullet \\ \hline \boldsymbol{A}(\omega_{\boldsymbol{P}}) \end{bmatrix} \begin{bmatrix} \Delta \boldsymbol{c}_1 \\ \cdot \\ \cdot \\ \Delta \boldsymbol{c}_{\boldsymbol{M}} \end{bmatrix} \qquad (13)$$

where the left hand side is a vector made up of P sub-vectors $\Delta \boldsymbol{k}(\omega_p)$. Each of these sub-vectors represents the differences in wavenumbers at frequency ω_p . On the right hand side the matrices $A(\omega_p)$ are the kernels of the integral equations corresponding to the different frequencies. The vector on the right hand side is a vector of the corrections to the compressional wave speed of the layers and this is determined by solving the matrix equation (13).

4.3. DESCRIPTION OF EXPERIMENT

The main objective of the MOMAXV experiment was to evaluate the use of air launched buoys for estimating the sediment acoustic properties from data acquired by it. In this set of experiments the buoys were not air launched but were deployed from a ship. In an effort to compare and contrast the performance of the commercially developed buoy meant for use by the Navy for deployment from air with the one developed at WHOI in almost identical conditions both the buoys were co-located by securing them together by a rope. The buoys were separated by a distance of about 5 meters. The buoys were then deployed from the ship. While the buoys drifted, a source transmitting multiple tones was towed thus creating synthetic aperture by the relative motion between the source and receiver. In order to distinguish various buoys deployed during the experiment they were all given a name/ a number. In the experiment described here the WHOI buoy is named SHEMP and the commercial buoy given the number SB810.

The area of the experiment together with the bathymetry of the region and the track of the ship and the buoy (Shemp) are shown in the left panel of Figure 4.3.1. During the course of the experiment CTD were deployed to measure the sound velocity profile in the water column. The sound speed profile obtained from the CTD data and a linear fit to the profile from the CTD data are shown in the right panel of Figure 4.3.1.

The source towed by the ship was a J15 source. It transmitted tones at four frequencies i.e. 50 Hz, 75 Hz, 125 Hz and 175 Hz, The source was deployed at a nominal depth of 53 m. The depth of the source was recorded by a pressure sensor. The receiver in the buoy was set to be deployed to a depth of 61 m. The depth of the receiver in Shemp was monitored using a pressure sensor located at a depth of 1.5 m from it. A similar sensor on the commercial buoy failed to function.

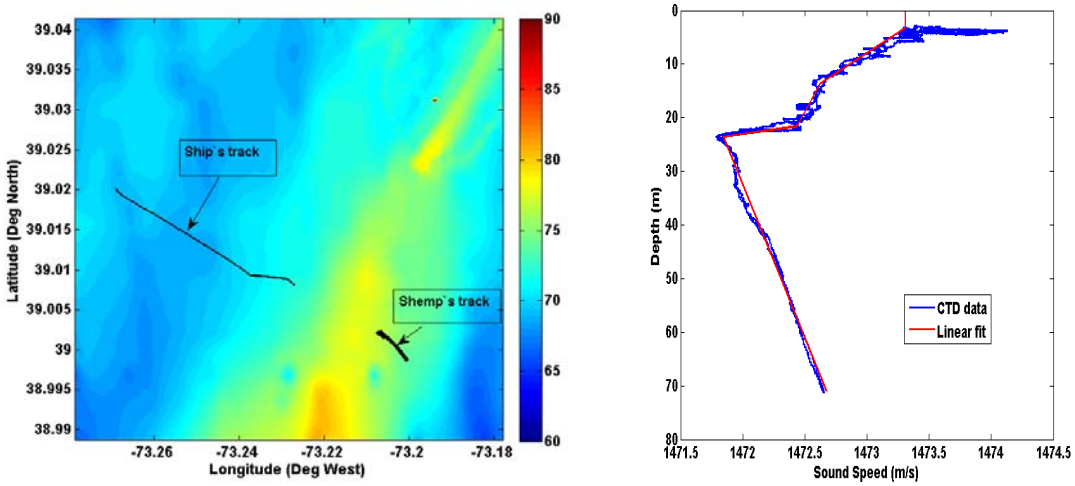

Figure 4.3.1. The left panel shows the general experimental area with the bathymetry of the region. The figure also shows the track of the ship and the position of the WHOI buoy (Shemp).

During the entire experiment, the location of the buoys and the ship were determined by the GPS units on the buoys and the ship. In the case Shemp it was recorded internally and recovered at the end of the experiment. In the case of the commercial buoy it was transmitted by an RF link to the towing ship. However, since the antenna on this buoy had a surface expression of only 2 feet, the GPS information was not reliable beyond a short range. However, since both the buoys were tied together the GPS data of Shemp buoy was assumed to be the same for SB810. The bathymetry along the track between the ship and the buoy at various times were determined and a mean bathymetry along the track between the ship and the buoy obtained. Figure 4.3.2 shows the bathymetry along the track at different times and the mean bathymetry.

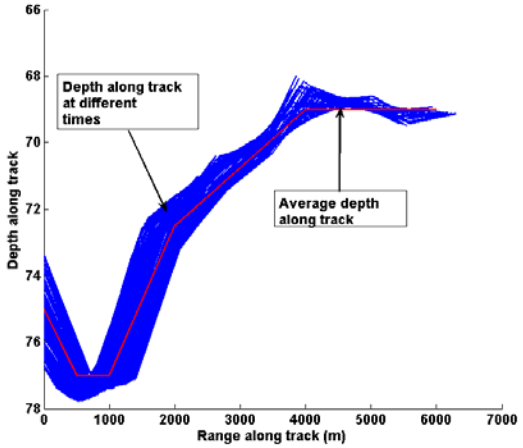

Figure 4.3.2. The bathymetry between the ship and the buoy at different times and the average bathymetry.

4.4. ESTIMATION OF EIGENVALUES

The tones are broadcast by the source continuously and the acoustic fields recorded at the receivers are therefore a function of time. The distances between the source and receiver at the times at the corresponding times are obtained from the GPS data. These two are merged to obtain the acoustic pressure field at the receiver as a function of range. The wave number spectrum is then obtained from the pressure field using (7). The pressure field at 50 Hz and the corresponding wavenumber spectrum for both Shemp and SB810 are shown in Figure 4.4.1.

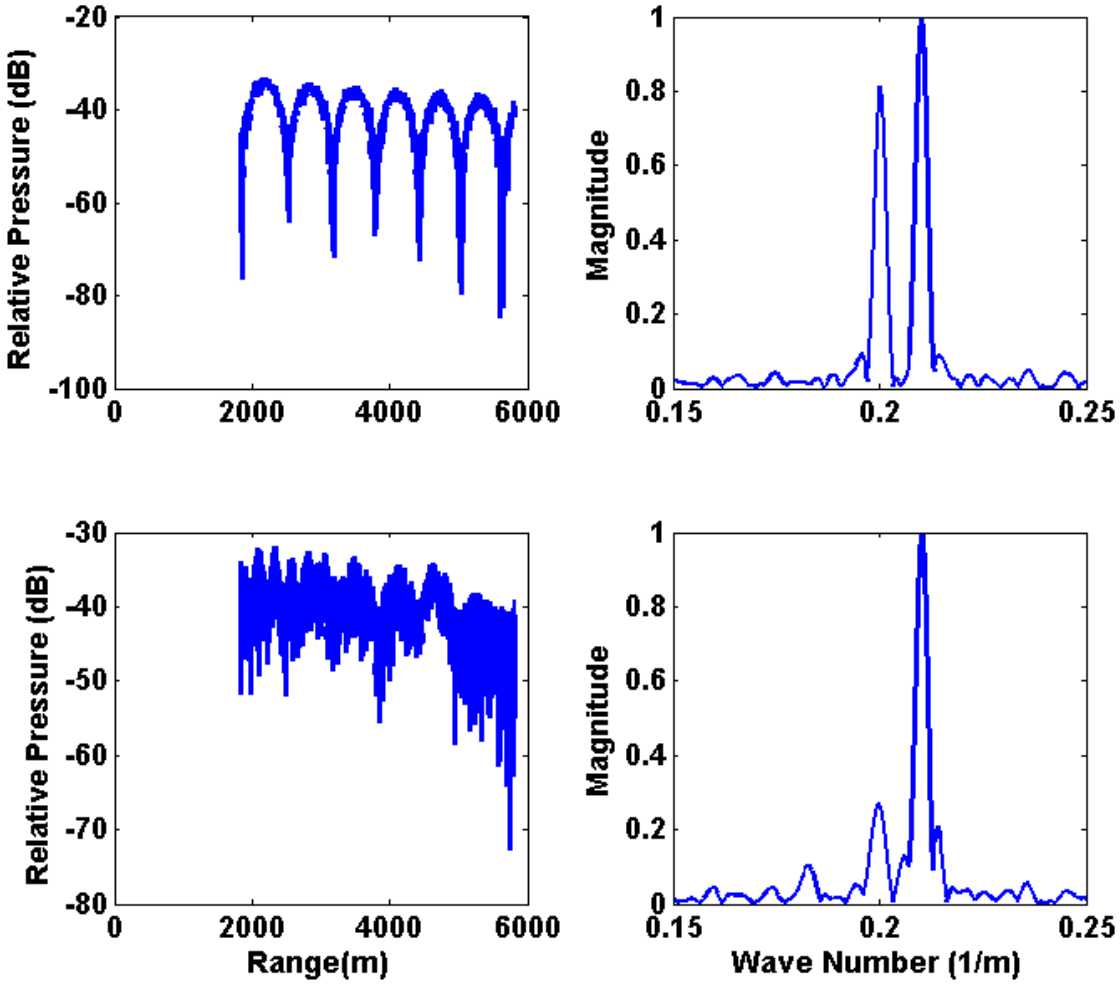

Figure 4.4.1. The top row shows the pressure field and the wave number spectrum for Shemp. The bottom row shows the pressure field and the corresponding wavenumber spectrum for the buoy SB810.

The pressure field data acquired by buoy SB810 are noisier than the data collected by buoy Shemp. The reason for this is not understood. However, the wavenumber spectrum in both cases show two dominant modes. The two mode interference pattern is evident in the field acquired by Shemp. In the case of SB810 it is masked by the noise in the data. It is also seen that relative mode amplitude of modes one and two are different while the eigenvalues corresponding to the location of these two modes are almost the same.

The data at other frequencies were similarly processed and the wave number spectrum obtained. The eigenvalues of modes were estimated from the wave number spectrum. These eigenvalues

were input to an inversion scheme and the bottom model obtained. The eigenvalues used in the inversion procedure are listed in Table 1.

Table 1: Eigenvalues estimate from data acquired by the two buoys

Frequency	Mode Number	WHOI buoy	Commercial buoy
50 Hz	1	0.2101553	0.2101617
	2	0.2001844	0.1998071
	3	0.1886796	0.1898359
75 Hz	1	0.3175340	0.3179272
	2	0.3102476	0.3106405
	3	0.2968252	0.2979848
	4	0.2818689	0.2853291
	5	0.2784175	0.2788095
	6	0.2584757	
125 Hz	1	0.5315243	0.5315405
	2	0.5269224	0.5269384
	3	0.5192683	0.5192683
	4	0.5104477	0.5073796
	5	0.4966262	0.4981754
	6	0.4924078	0.4947239
	7	0.4732331	0.4728640
175 Hz	1	0.7455146	0.7466879
	2	0.7420632	0.7424693
	3	0.7359272	0.7351827
	4	0.7324758	0.7282796
	5	0.7156020	0.7175414
	6	0.7029467	0.7060362
	7	0.6864564	0.7029681
	8	0.6833884	0.6868608
	9	0.6680486	0.6699865

4.5. INVERSION FOR SEDIMENT COMPRESSIONAL WAVE SPEED PROFILE

Inversion from the compressional wave speed in the sediment layers was done using the matrix equation (13). This equation represents Fredholm integral equation of the First kind. These equations are inherently ill conditioned and solutions are therefore obtained by constraining the solution. Here we adopt qualitative regularization [9] to obtain a solution to the matrix equation. In the case of layered medium this method of regularization in addition to applying to smoothness constraint in the layers it also provides the ability to incorporate in the solution a priori information on interface depth between layers where discontinuities in sediment properties can occur. Further in the case of modes which are not strong it was assumed that they have

larger variance and this information was also incorporated in solving the inverse problem. If even with these constraints the inverse of the matrix is found to be ill conditioned a small quantity was added to the diagonal of the matrix being inverted to make the matrix well conditioned.

The following assumptions were made in performing the inversion.

1. The sediment layers are assumed to be fluid.
2. The density and attenuation of the sediment layers are assumed to have a constant value in each sediment layer and in the termination half space. These values are assumed to be known. The acoustic field in the water column is most sensitive to the compressional wave speed of the sediments and water column and its sensitivity to sediment density and attenuation is small in comparison. Therefore errors in the assumed values of density and attenuation of the sediment layers will not affect the estimates of the sediment compressional wave speed.
3. Attenuations in the sediment layers and in the half space were ignored.
4. The density values in all the sediment layers and in the half space were set at 1.6 gm/cc.
5. The compressional wave speed of 1850 m/s was assumed for the half space. This was based on the highest value of the turning speed obtained from the eigenvalues. The turning speed is given by $\frac{2\pi f}{k_n}$ where f is the frequency and k_n the eigenvalue of the nth mode.

The sediment was assumed to consist of 32 layers each with a thickness of one meter. It was also assumed that the discontinuities occurred at a depth of 8 m and 23 m from the ocean bottom. To arrive at the location of the discontinuities the following procedure was adopted. First inversion was performed without enforcing the constraint on discontinuities. The result showed that the compressional wave speed increased from a low value, reached a maximum and the reduced to a lower value. Further the archival information available for the region in proximity to the experimental area indicated a top layer of approximately 10 m. The locations of discontinuities were varied to obtain a model that was best in predicting the measured pressure field. This resulted in the location for the discontinuities indicated above.

Inversions were done using the eigenvalues of modes at all the frequencies in a multi-frequency inverse as indicated in (12). The compressional wave speed of the sediment layers as obtained from the inversion are shown in Figure 4.5.1. It is observed that data from both the buoys yield the compressional wave speed profile of the sediment layers which are close to each other.

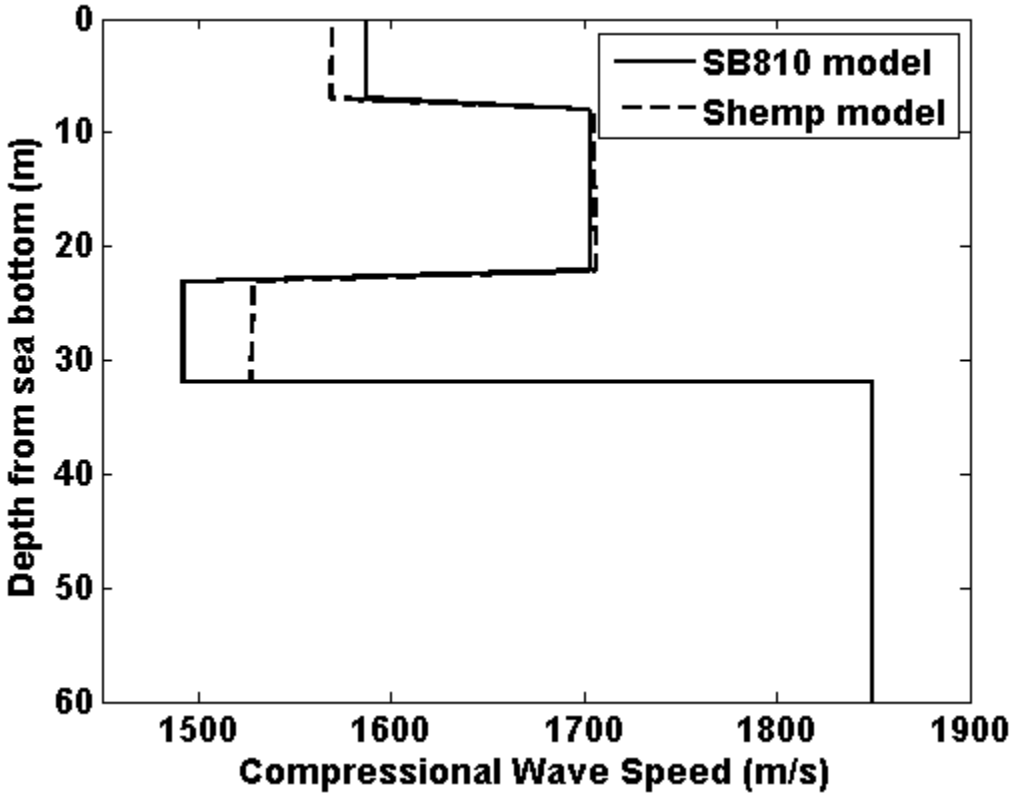

Figure 4.5.1. The compressional wave speed profile of the sediment layers as obtained from inversion of the data from Shemp and SB810.

4.6. VALIDATION OF RESULTS

4.6.1. Verification of Model from Chirp Sonar Survey and Other Inversions

A high resolution chirp sonar survey was conducted in the general area of the Shallow Water Experiment 2006. This survey indicated that the sediment consists of an upper layer, a lower layer and reflective interface beneath it. Over the years a number of experiments were conducted in the area and different inversion methods were used to extract the compressional wave speed profiles in the three regions. Average values for the three layers as obtained from these experiments are listed below.

Table 2: Average compressional wave speed in the three region delineated by chirp sonar survey.

Location	Compressional wave speed (m/s)
Upper layer	1658.0
Lower layer	1578.0
Below reflector	1734.0

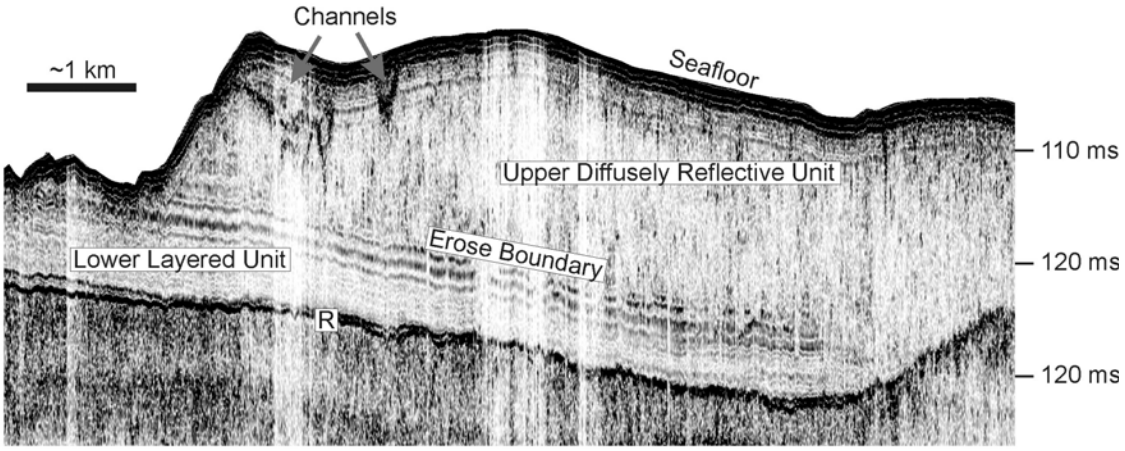

Figure 4.6.1. Chirp seismic section measured during SW06 with prominent features identified. The \R" reflector is indicated by dark line near bottom of figure. (Figure from [10]).

The region of experiment conducted in 2011 as shown in Figure 4.3.1 falls in a region where the upper layer is absent as seen at the left end of Figure 4.6.1. In this region the top surface is the lower layer and beneath that is the reflector. The chirp sonar survey does not provide any information of the layering beneath the reflector. However model obtained for a location in the area of Shallow Water Experiment 2006 suggests the presence of a low velocity region beneath the reflection interface [11]. These corroborate the bottom model obtained by the inversion of data acquired by both Shemp and SB810.

4.6.2. Comparison of Eigenvalues

The eigenvalues estimated from experimental data are compared with the eigenvalues of the inverted model. This comparison is made in Figures 4.6.2 and 4.6.3.

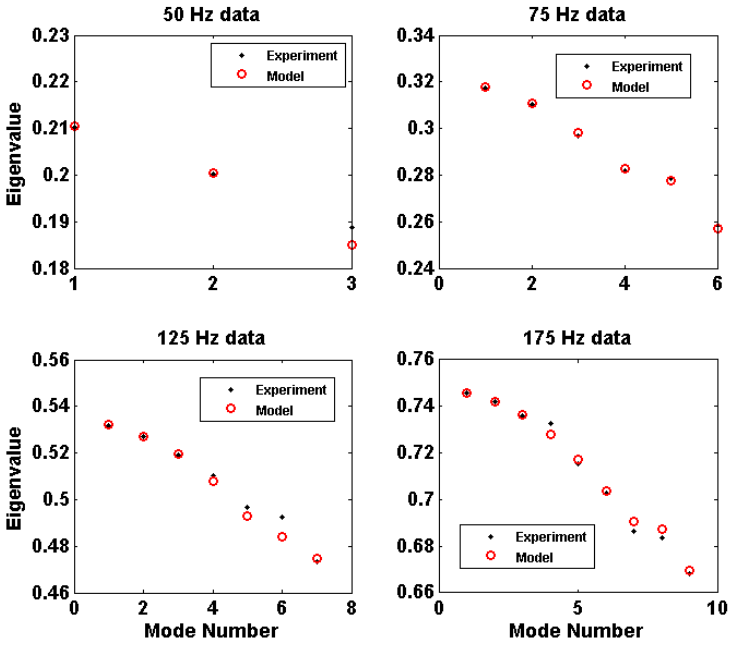

Figure 4.6.2. The figure shows the agreement between the eigenvalues estimated from data and the eigenvalues of the model in the case of Shemp.

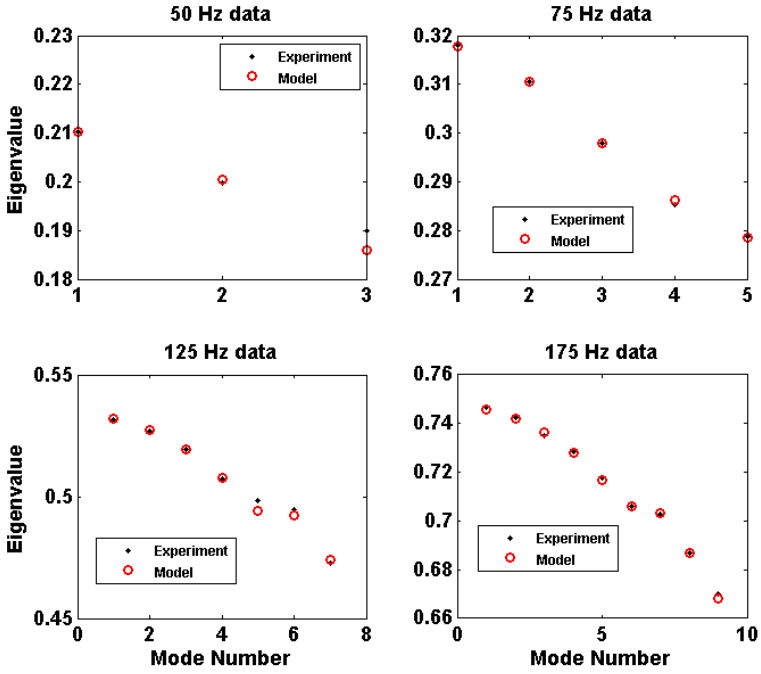

Figure 4.6.3. The plots show the agreement between the eigenvalues from data and the eigenvalues from the model for SB810.

4.6.3. Prediction of Transmission Loss

The sediment model obtained by inversion is now used in conjunction with a propagation model to predict the transmission loss. It is seen from Figure 4.3.2 that the bathymetry varies along the track. The variation of bathymetry along the track is shown in Table 3.

Table 3: Range dependent bathymetry along the track between source and receiver

Range (km)	0.0	0.5	1.0	2.0	4.0	6.0
Depth (m)	75.0	77.0	77.0	72.5	69.0	69.0

The transmission loss was computed using adiabatic mode theory that incorporated the range dependence of bathymetry as given in Table 3.

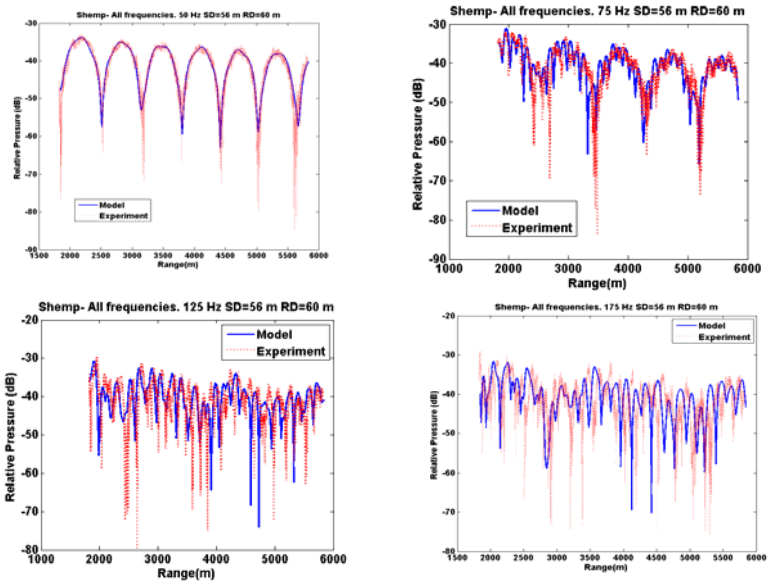

Figure 4.6.4. The four plots in the figure compares the transmission loss obtained from experimental data with the transmission loss predicted by the Shemp model. The four plots are for the four frequencies broadcast during the experiment.

To compute the transmission loss, the density in the sediment layer and the half space was set at 1.6 gm/cc. Attenuation in the layers was set at 0.05 dB/K/m. We see from Figures 4.6.4 and 4.6.5 that the models obtained by Shemp and SB 810 are able to predict the transmission loss measured during the experiments. These results further confirm the conclusion that the bottom models obtained by inversion process are consistent with the experimental measurements.

It is seen from Figure 4.4.1 that the Green's function at 50 H for Shemp and SB810 have eigenvalues at almost identical location on the wavenumber axis however their amplitudes are

different. A likely cause for this is the discrepancy in the location of the receiver/source. Since the source location for both Shemp and SB810 is the same, the difference can be due to receiver location. Even though the receiver of SB 810 was set to be at a depth of 61 m as in the case of Shemp, it is felt that due to the fact that SB 810 was attached and being dragged by Shemp, the receiver of SB810 kited to a depth of 49 m. This is the depth at which there is good agreement between the Green's functions of measured data and the data from the model prediction of the field by SB810. Therefore all computation for transmission loss for SB810 was done using a source depth of 56 m and a receiver depth of 49 m for SB810. In the case of Shemp the source depth was 56 m and the receiver depth was set at 60 m.

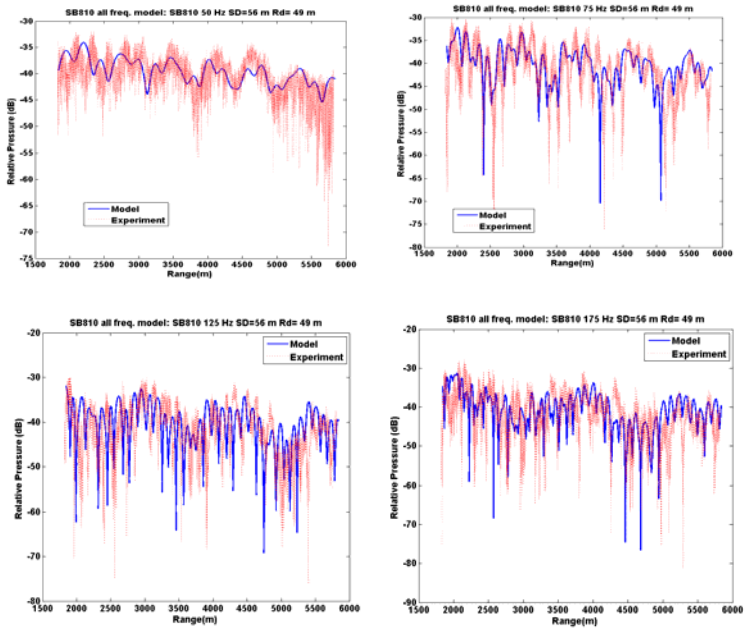

Figure 4.6.5. The four plots compare the transmission loss as measured by SB 810 during the experiment with the transmission loss computed using SB 810 bottom model.

5.0. CONCLUSION

We have studied the inversion algorithm for estimating the sound speed profiles in a range dependent environment. The method is based on representing the range-dependent environment as a set of range-independent sections. Two approaches are investigated. In one approach we study the use of extended Kalman filter to extract range dependent sound speed profiles. In this case CW signals are transmitted and the signals are acquired in a vertical array of receivers. The extended Kalman filter is then adopted to extract the range dependent sound speed profiles. The Kalman filter approach is essentially identical to an inverse procedure where the non-linear problem is linearized and then inversion attempted as for a linear problem. These methods can be used to extract range dependent sound speed profiles**.** The second approach is the use of mode travel time. It was shown that in the case of range-dependent sound speed profiles of the water

column the profiles can be obtained by collecting data from multiple source/receiver combinations. We demonstrated the performance of this method using synthetic data. The study with synthetic data showed that even when there is mode coupling present it is possible to use data from frequencies where the mode coupling is absent and invert for the sound speed profile in the water column. This suggests that it is necessary to design the signaling scheme such that the frequency band of the transmitted signal provides adequate usable data for performing the inverse.

The results of analysis from data collected by two types of sonobuoys show that the consistent bottom model can be obtained by analysis of the acquired data. Analyses of data from two other deployments of sonobuoys (Larry and SB098 and Larry and SB795) show that bottom model estimates from both types of buoys are consistent. These results are not included in this report as no new additional inferences are obtained from these analyses. This analysis allows the exploitation of schemes for estimating geoacoustic properties from air launched buoys used in ASW operations.

6.0. REFERENCES

[1] Olivier Carriere, Jean-Pierre Hermand, Jean-Claude Le Gac, and Michel Rixen," Full field tomography and Kalman tracking of the range dependent sound speed field in a coastal environment, Journal of Marine Systems, S382-S392, 2009.

[2] S. D. Rajan and K. M. Becker," Inversion for range-dependent sediment compressional wave speed profiles from modal dispersion data," IEEE Journal of Oceanic Engineering, 35(1), 43-55, 2010.

[3] S. D. Rajan, F068-N00014-10-C-0772-CDRL0001AA Progress report submitted to ONR, March 2011.

[4] Kyle M. Becker and G.V. Frisk, "The impact of water column variability on horizontal wave number estimation and mode based geoacoustic inversion results," Journal of the Acoustical Society of America, 123, 658-666, 2008.

[5] M. D. Collins, "A split-step Pade solution for the parabolic equation method," Journal of the Acoustical Society of America, 93, 1736-1742, 1992.

[6] Scott D. Frank, Mohsen Baidey, James F. Lynch and William L. Seigmann," Analysis and modeling of broadband air gun data influenced by nonlinear internal waves," Journal of the Acoustical Society of America, 116, 3404-3422, 2004.

[7] George V Frisk and James F Lynch," Shallow water characterization using Hankel transform," Journal of the Acoustical Society of America, 76, 205–211, 1980.

[8] S. D. Rajan, J. F. Lynch, and G. V. Frisk, "Perturbative inversion methods for obtaining bottom geoacoustic parameters in shallow water," Journal of the Acoustical Society of America, 82(3), 998-1017, 1987.

[9] Megan S. Ballard and Kyle M. Becker," Optimized constrains for the linearized geoacoustic inverse problem, Journal of the Acoustical Society of America, 129(20), 652-661, 2011.

[10] Megan S. Ballard, Kyle M. Becker and John A. Goff, "Geoacoustic inversion for the New Jersey shelf: 3-D sediment model," IEEE Journal of Oceanic Engineering, 35(1), 28-42, 2010.

[11] Cederberg, R.J., W.M. Carey, and W.L. Siegmann, "Modal analysis of geoacoustic influences on shallow water propagation," IEEE Journal of Ocean Engineering, 22(2), 237-244, 1997.

DISTRIBUTION LIST

Addressee	DOD AAD CODE	Number of copies
Kyle Becker, PhD Code: 322OA Office of Naval Research (ONR) 875 North Randolph Street, Suite 1425 Arlington, VA 22203-1995 REF: N00014-10-M-0072 Email: kyle.becker1@navy.mil	N00014	1 (Emailed)
Administrative Contracting Officer Email notification only to: marianne.delgreco@dcma.mil	S2206A	1 (Transmittal Letter Only)
Defense Technical Information Center 8725 John J. Kingman Rd, Suite 0944 Ft. Belvoir, VA 22060-6218 Email: TR@DTIC.mil	HJ4701	1 (Emailed)
Director, Naval Research Lab ATTN: Code5596 4555 Overlook Avenue, SW Washington, DC 20375-5320 Email: reports@library.nrl.navy.mil	N00173	1 (Emailed)
Scientific Solutions, Inc. 99 Perimeter Road Nashua, NH 03063-1325	Cage Code: 0VH19	1 (Contract Files)